

MIT Open Access Articles

VARIABILITY OF PLASMA IN THE HELIOSHEATH

The MIT Faculty has made this article openly available. **Please share** how this access benefits you. Your story matters.

Citation: Richardson, J. D. "VARIABILITY OF PLASMA IN THE HELIOSHEATH." The Astrophysical Journal 740, no. 2 (October 4, 2011): 113. © 2011 The American Astronomical Society

As Published: <http://dx.doi.org/10.1088/0004-637x/740/2/113>

Publisher: IOP Publishing

Persistent URL: <http://hdl.handle.net/1721.1/95669>

Version: Final published version: final published article, as it appeared in a journal, conference proceedings, or other formally published context

Terms of Use: Article is made available in accordance with the publisher's policy and may be subject to US copyright law. Please refer to the publisher's site for terms of use.



VARIABILITY OF PLASMA IN THE HELIOSHEATH

J. D. RICHARDSON¹

Kavli Center for Astrophysics and Space Research, Massachusetts Institute of Technology, Cambridge, MA 02139, USA; jdr@space.mit.edu

Received 2011 June 3; accepted 2011 July 28; published 2011 October 4

ABSTRACT

The heliosheath is the shocked solar wind between the termination shock and the heliopause. Plasma properties are highly variable in this region, with factor-of-two variations of density and thermal speed on timescales from tens of minutes to hours to days. Gaussian distributions fit all the heliosheath plasma data well and are used to quantify these variations. We show that these fits can be used to compensate for data lost due to cutoffs in the instrument response and show that the flow angle in the RT plane is about 50% larger than previous determinations. The turbulent component of the flow has about 25% of the flow energy in the heliosheath, but this energy is not a significant percentage of the upstream solar wind flow energy.

Key words: interplanetary medium

Online-only material: color figures

1. INTRODUCTION

The heliosheath (HSH) is the region of shocked solar wind between the termination shock (TS) and the heliopause. It comprises the majority of the heliosphere by volume. The solar wind is heated and compressed at the TS so that the HSH flow is subsonic and diverts down the heliotail. Sheaths are very turbulent regions, with variations generated in the upstream flow, at the shock, and in the sheath (Shevyrev et al. 2003). The variations in the plasma parameters observed by *Voyager 2* (V2) decrease beginning in late 2008, when V2 had been in the HSH about one year. This decrease may result from V2's increasing distance from the TS; models show that in late 2008 the TS started moving inward in response to a decrease in solar wind pressure (Richardson & Wang 2011).

The magnetic field in the HSH is highly variable on timescales from 48 s to days (Burlaga et al. 2006; Burlaga & Ness 2009a). Field fluctuations of factors of two to four are common. The distribution of the magnetic field strength is Gaussian in some regions and log-normal in others at both V1 and V2. At V2, the region near the TS from 2007.7 to 2008.6 has a log-normal distribution and the region from 2008.6 to 2009.4 has a Gaussian distribution (Burlaga & Ness 2009a).

This paper discusses the variability of the plasma parameters in the HSH. The plasma distributions and their time evolution are presented. These distributions are used to correct for systematic errors in the plasma flow angles caused by cutoffs in the instrument response. The HSH fluctuations are compared with those observed at Jupiter.

2. THE DATA

The *Voyager* plasma experiment (PLS) observes ions in the HSH with energy/charge from 10 to 5950 eV q^{-1} in four modulated-grid Faraday cups (Bridge et al. 1977). Three of these cups are arranged in a cone whose central angle points toward Earth, roughly into the direction of the HSH flows. The face of each of these three detectors is tilted 20° from the cone axis. The instrument response is nearly flat for ions entering the cups

within 45° of the cup normal. From 45° to 60° the instrument response falls roughly linearly to zero. The time resolution is 192 s in the HSH.

We select times when V2 observes currents in all three Earthward-looking detectors and fit these data with convected isotropic proton Maxwellian distributions to determine the plasma velocity, density, and temperature; these distributions generally provide good fits to the observations. If the uncertainties in the fits are large, in particular if the uncertainty in $N > N$, the fit is rejected. Peak ion currents are typically 10^{-14} – 10^{-13} A; the lower values are close to the noise level of the instrument. The uncertainties introduced by this noise contribute to 1σ error bars for the fit parameters of about 10% for V_R , 30% for N , and 40% for the thermal speed W_{TH} . We derive plasma parameters for about 20,000 spectra, roughly 10% of the available spectra. For the rest of the spectra the above criteria are not met, sometimes because densities or flow angles are beyond the instrument threshold but mostly because of noise. We use the standard RTN coordinate system, where R is radially outward, T is parallel to the solar equator and positive in the direction of solar rotation, and N completes a right-handed system.

Figure 1 shows the plasma speed, density, thermal speed, and flow angles from each set of spectra with five-day running averages superposed. The gap in 2010 was caused by a spacecraft malfunction. Daily averages of the HSH data through 2011.2 and a description of these data are published (Richardson & Wang 2011). A new feature in the most recent data is a 30%–40% increase in the average density starting at about 2011.2. This increase is likely due to solar wind conditions changing as we leave solar minimum. We note that a recent heliosphere model (Washimi et al. 2011) predicts a rise in density in a “plasma-pause” near the heliopause similar to that observed. However, this model also predicts that the heliopause is 20 AU beyond V2's current location so a solar source for this increase seems more likely.

Figure 1 shows that all the plasma parameters have large variations about the mean on timescales down to minutes. The amplitude of these variations can be factors of two to three and are larger near the TS. These fluctuations seem to be real as the underlying spectra are observed to change significantly on timescales of tens of minutes, similar to the timescales for magnetic field fluctuations.

¹ Also at State Key Laboratory for Space Weather, Chinese Academy of Sciences, Beijing, China.

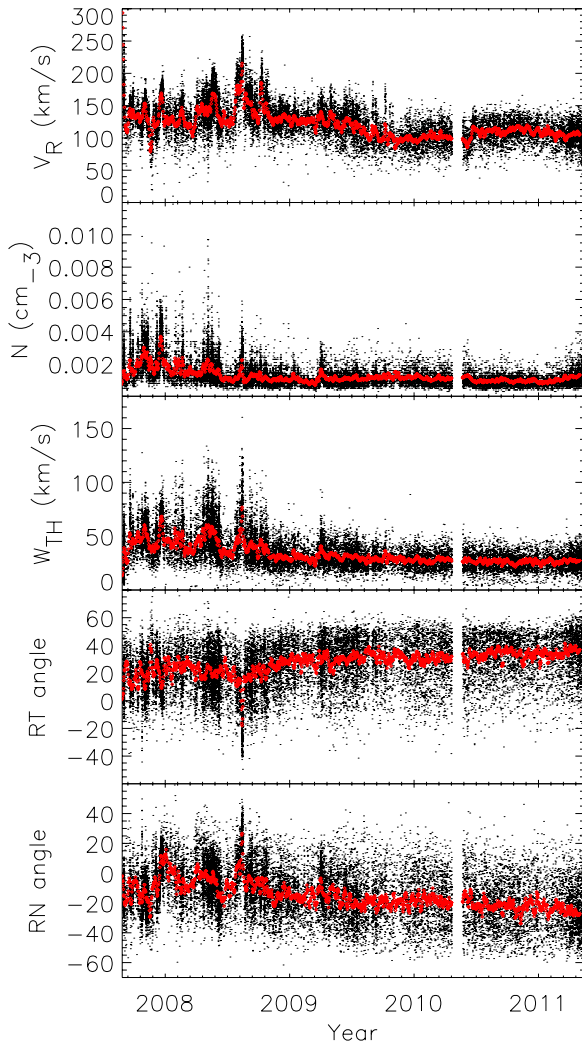


Figure 1. Plasma parameters in the HSH with five-day running averages superposed.

(A color version of this figure is available in the online journal.)

Figures 2–6 show histograms of the distributions of the plasma parameters in the HSH for each year from 2007 to 2011. Figure 2 shows the distribution of V_R in 1 km s^{-1} bins; the abscissa shows the percentage of points in each bin. We fit the data with a Gaussian distribution of the form

$$F = Ae^{-(V-B)^2/2W^2}, \quad (1)$$

where B is the average speed and W is the width of the distribution. The speed distributions are clearly Gaussian. The speed decreases from an average of 145 km s^{-1} in 2007 to 106 km s^{-1} in 2011. The distribution is narrower by about 7 km s^{-1} in 2011 than in 2007.

Figure 3 shows the density histogram in 10^4 cm^{-3} bins. A Gaussian distribution fits the data well in 2007 but in subsequent years a tail is present at higher densities. Models show that shocks driven by merged interaction regions (MIRs) can drive density pulses through the HSH (Zank & Mueller 2003; Washimi et al. 2011); these pulses could be the cause of the high-density tail of the distribution. At lower densities a Gaussian distribution fits the data reasonably well, suggesting that the cutoff in density due to the instrument response is not important. The density decreases with time and the width of the distribution becomes smaller with time.

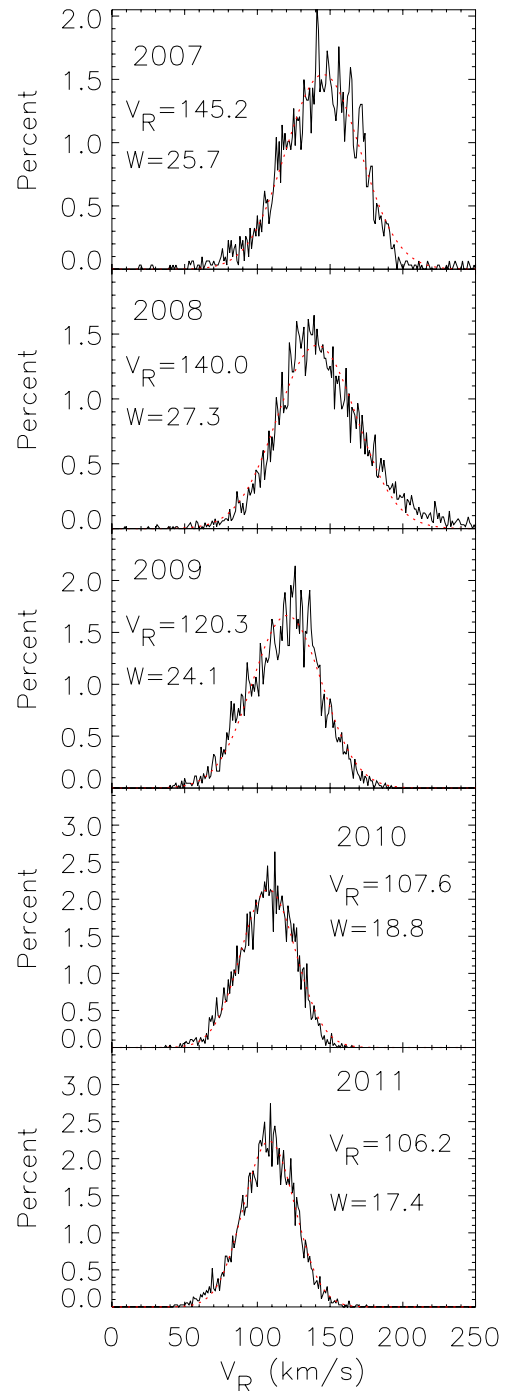


Figure 2. Histogram of the distribution of V_R in the HSH plotted in 1 km s^{-1} bins by year. Superposed are Gaussian fits to these data.

(A color version of this figure is available in the online journal.)

Figure 4 shows the distribution of the thermal speeds in 1 km s^{-1} increments. These distributions are well fitted by Gaussians every year but 2008, when a larger than Gaussian tail at high thermal speeds and a cutoff at low thermal speeds were observed. The thermal speed decreases with time as does the width of the distribution.

Figure 5 shows the distribution of plasma flow angles in the RT plane in 1° bins with zero corresponding to radial flow. The fit to a Gaussian is quite good in 2007 when the average angle was 16° . However, as time progresses and the average angle increases a cutoff is observed in the data starting between 45°

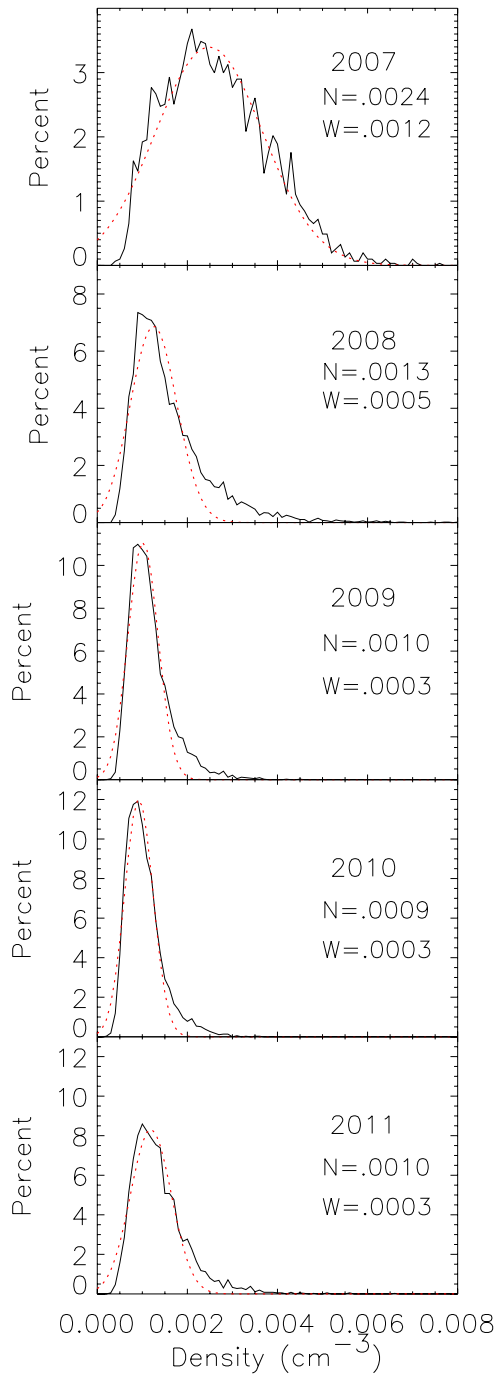


Figure 3. Histogram of the distribution of density in the HSH plotted in 10^4 cm^{-3} bins by year. Superposed are Gaussian fits to these data.
(A color version of this figure is available in the online journal.)

and 50° . This effect is moderate in 2008 but increases with time. This cutoff is probably due to the instrument response, which decreases when the angle between the flow and the cup normal is over 45° and goes to zero when this angle is over 60° . This cutoff means that large angle flows are not observed in all three detectors so that the plasma analysis is not performed. The exact cutoff angle depends on the plasma density and thermal speed. The Gaussian fits to the RT angle distributions use only data with RT angles less than 50° , so they are not affected by this cutoff.

Figure 6 shows the RN angle histogram and Gaussian fits. The RN angles are smaller than the RT angles throughout the

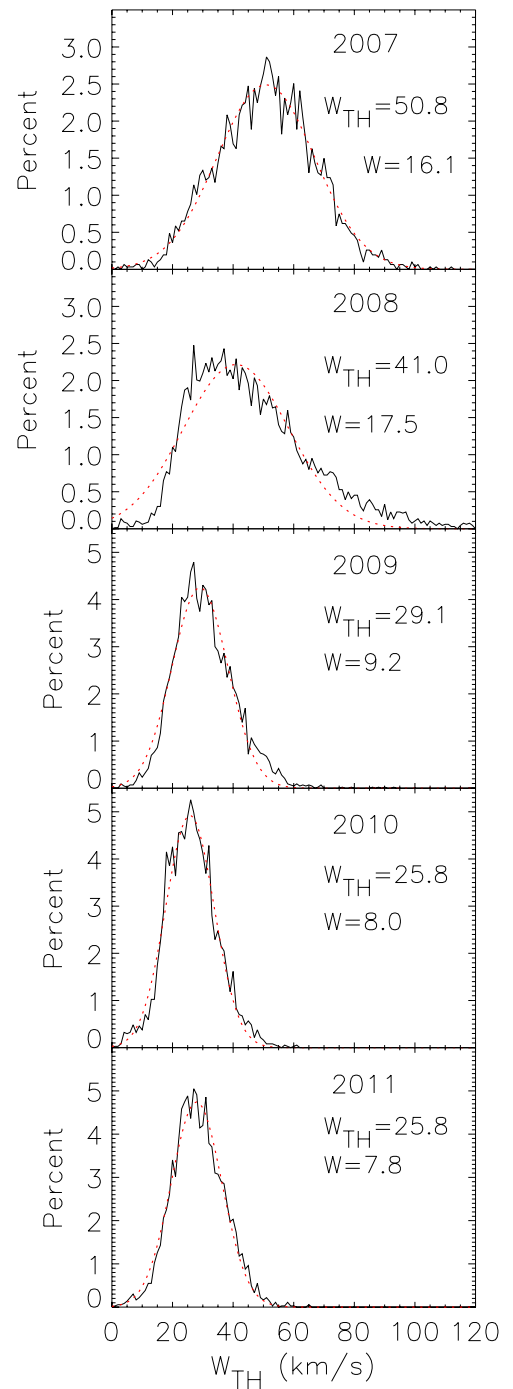


Figure 4. Histogram of the distribution of the thermal speed in the HSH plotted in 1 km s^{-1} bins by year. Superposed are Gaussian fits to these data.
(A color version of this figure is available in the online journal.)

HSH. The RN angles do get larger with time, indicating more southward flow, but the flow angles seem not to be affected by the instrumental cutoff until 2009, and then to a much lesser extent than RT . From 2009 to 2011 the tail of the distribution is less than the Gaussian fit predicts, but the main part of the distribution is not affected by the cutoff.

The widths of the RT and RN angle distributions do not change in time whereas the width of the V_R distribution decreases with time. This indicates that the velocity fluctuations in the T and N directions are proportional to V_R , perhaps suggesting vortical flow generated by TS motions (Washimi et al. 2011).

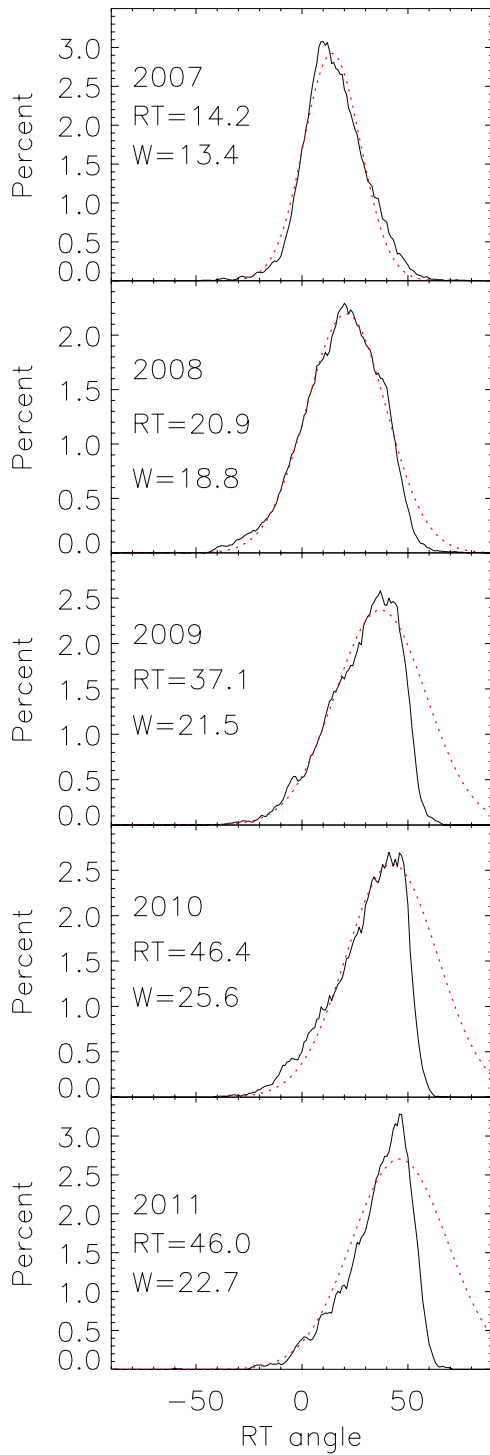


Figure 5. Histogram of the distribution of the RT angle in the HSH plotted in 1° bins by year. Superposed are Gaussian fits to these data.

(A color version of this figure is available in the online journal.)

3. DISCUSSION

The *Voyager* spacecraft are providing the first in situ data from the HSH and it is likely that many years will pass before future spacecraft follow their lead. Since the *VI* plasma instrument is not working, we rely on *V2* for high-resolution plasma parameters. One obstacle to making these observations is the instrument limitations. Densities below about 0.0004 cm^{-3} are difficult to measure. The detector response to flow angles greater

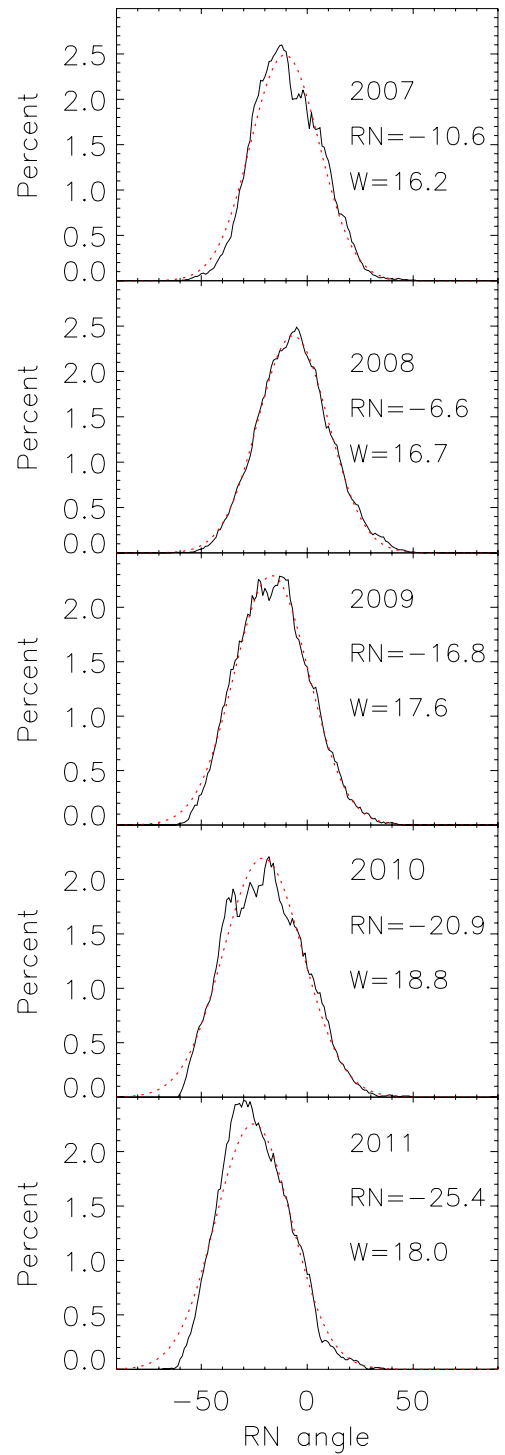


Figure 6. Histogram of the distribution of the RN angle in the HSH plotted in 1° bins by year. Superposed are Gaussian fits to these data.

(A color version of this figure is available in the online journal.)

than 45° to the cup normals is reduced and goes to zero for flow angles greater than 60° . Since the detectors are tilted 20° to the radial direction, some signal will be observed in at least one detector for flow angles up to 80° from the radial direction, but full vector plasma velocities cannot be determined for angles above 50° from the radial direction. When currents are not observed in all three detectors, it is more difficult to differentiate signal from noise.

We note above that Figure 3 implies that low densities are not yet a limiting measurement factor since we observe most of the Gaussian distribution of the densities. Solar minimum is expected to have the lowest densities at the V2 heliolatitude of -29° (since at solar minimum the admixture of low-density, high-speed stream material is largest). Solar minimum conditions reached V2 in early 2011, so the plasma densities are expected to increase. That increase may have started at 2011.2 as shown in Figure 1.

Figure 5 shows that the RT angle distributions are affected by the instrumental cutoff, in that flow angles are too large for the plasma to be observed in all three cups in a significant fraction of the spectra. The flow angles are expected to continue to increase as the plasma continues to divert tailward. The high variability of the HSH flows helps with this problem. All the plasma parameters have reasonably Gaussian distributions. The width of these distributions is fairly large due to the highly variable nature of the HSH. For the Gaussian fits to the RT angle the widths of the distribution are 13, 19, 22, 22, and 23 km s^{-1} for 2007–2011. The widths of the RN angles are 16, 17, 18, 19, and 18 km s^{-1} . By assuming that the widths are constant one can constrain the Gaussian fit parameters for the average angle and thus determine the flow velocity even when a substantial portion of the distribution is lost because of the instrument response.

We use these distributions to correct the RT angle for the instrument cutoff. The RT angles derived by averaging all the angles in each year from 2007 to 2011 are 15° , 19° , 30° , 31° , and 33° . The average RT angles derived from the Gaussian fits are 14° , 21° , 37° , 46° , and 46° . The instrument cutoff clearly affects the average RT angle derived from the data after 2008; the 2010 and 2011 flow angles derived from the fits are about 46° , which is 13° higher than the flow angle derived by simply averaging the data. For comparison, the RN angles derived by averaging all the angles in each year are -9° , -6° , -15° , -19° and -23° , which are comparable to the fit results of -11° , -7° , -17° , -20° , and -25° . This result shows that the RN angles observed to through mid-2011 are only slightly biased by the instrumental response.

That the RT angle is larger than the RN angle has been a puzzle. One hypothesis is that the shock is blunter in the RT than RN planes in *Voyager*'s direction, causing a larger flow rotation in the RT plane at the shock (Richardson et al. 2009). However, models have found that the radius of curvature is slightly smaller in the RT than in the RN planes (Borovikov et al. 2011). Another possibility is that the plasma is being compressed and moving along the magnetic field; the magnetic pressure is increasing across the HSH (Burlaga et al. 2009b) if changes at the Sun are accounted for. The three-dimensional MHD model of Borovikov et al. (2011) predicts matched the RN and RT angles from previous data analyses fairly well; however, the increased values of the RT angle reported here are not consistent with these model results.

For comparison, we performed similar Gaussian fits to the Jovian dayside magnetosheath plasma data. The parameters that are most analogous between the HSH and magnetosheath are V_T and V_N . V_R (and thus the flow angles) are driven by changes in the magnetosheath boundary locations, which are large and rapid when scaled to those of the HSH. A large fraction, 30%–50%, of the ions in Jupiter's magnetosheath are reflected thermal ions (Richardson 2002). In the HSH, the plasma pressure is dominated by pickup ions. These pickup ions are reflected at the TS and gain most of the energy dissipated at the TS (Zank et al. 1996; Richardson et al. 2008). Thus, density and

thermal speed distributions at Jupiter and in the HSH cannot be directly compared. For the HSH, the width of the V_T and V_N distributions are 47 and 48 km s^{-1} , respectively. For the Jovian magnetosheath, the distributions were narrower, 21 km s^{-1} for V_T and 30 km s^{-1} for V_N . Thus, velocity disturbances created at the TS and/or in the HSH are greater than those in the smaller Jovian magnetosheath, perhaps due to generation of vortexes at the TS (Washimi et al. 2011).

The fluctuations in speed are superposed on the average flow. Thus, an energy budget for the heliosphere needs to include this turbulent component of the flow. Only about 15% of the flow energy of the solar wind went into heating the thermal plasma at the TS and about 5% went to the observed higher-energy ions. The average of the turbulent speeds using the width of V_R from Figure 2 and of V_T and V_N from the preceding paragraph is about 70 km s^{-1} , compared with the average speed of 144 km s^{-1} for all HSH data. Thus, about 24% of the flow energy in the HSH is in the turbulent flow component, or $<5\%$ of the flow energy in the upstream solar wind. Most of the upstream flow energy likely goes into heating the pickup ions (Zank et al. 1996; Richardson et al. 2008).

4. SUMMARY

We describe the distributions of plasma parameters in the HSH. These distributions are generally well fitted by Gaussians. Recent data show an increase in density, perhaps related to the ascending phase of the solar cycle. The variability of N , T , and V_R (as determined from the width of the distributions) decrease as V2 moves deeper in the HSH. The distributions of V_T show that the limited angular field of view of the instrument results in a cutoff of the RT angles above 50° . Fitting the distribution to a Gaussian shows that the average RT angle is 46° in 2010 and 2011, 13° – 15° larger than previous values, so that the flow angles in the RT plane are almost twice those in the RN plane. Although the turbulent flows are large compared with other plasmas, they comprise only a small amount of the upstream solar wind flow energy.

This work was supported under NASA contract 959203 from the Jet Propulsion Laboratory to the Massachusetts Institute of Technology and NASA grant NNX08AE49G and grant NNSFC 40921063 and by the Specialized Research Fund for State Key Laboratories of China.

REFERENCES

- Borovikov, S. N., Pogorelov, N. V., Burlaga, L. F., & Richardson, J. D. 2011, *ApJ*, **728**, L21
- Bridge, H. S., Belcher, J. W., Butler, R. J., et al. 1977, *Space Sci. Rev.*, **21**, 259
- Burlaga, L. F., & Ness, N. F. 2009a, *ApJ*, **703**, L311
- Burlaga, L. F., Ness, N. F., Acuña, M. H., et al. 2009b, *ApJ*, **692**, 1125
- Burlaga, L. F., Ness, N. F., & Acuña, M. H. 2006, *ApJ*, **642**, 584
- Richardson, J. D. 2002, *Planet. Space Sci.*, **50**, 503
- Richardson, J. D., Kasper, J. C., Wang, C., Belcher, J. W., & Lazarus, A. J. 2008, *Nature*, **464**, 63
- Richardson, J. D., Stone, E. C., Kasper, J. C., Belcher, J. W., & Decker, R. B. 2009, *Geophys. Res. Lett.*, **36**, L10102
- Richardson, J. D., & Wang, C. 2011, *ApJ*, **734**, L21
- Shevryev, N. N., Zastenker, G. N., Nozdachev, M. N., et al. 2003, *Adv. Space Res.*, **31**, 1389
- Washimi, H., Zank, G. P., Hu, Q., et al. 2011, *MNRAS*, **416**, 1475
- Zank, G., Pauls, H., Cairns, I., & Webb, G. 1996, *J. Geophys. Res.*, **101**, 457
- Zank, G. P., & Mueller, H. R. 2003, *J. Geophys. Res.*, **108**, 1240